d-wave superconductivity in narrow-band systems: the effect of second-nearest-neighbour hopping, the isotope effect, and the pressure effect

1997 J. Phys.: Condens. Matter 9 3889

(http://iopscience.iop.org/0953-8984/9/19/010)

J. Phys.: Condens. Matter **9** (1997) 3889–3900. Printed in the UK PII: S0953-8984(97)79379-2

d-wave superconductivity in narrow-band systems: the effect of second-nearest-neighbour hopping, the isotope effect, and the pressure effect

S Sil and A N Das

Saha Institute of Nuclear Physics, 1/AF Bidhannagar, Calcutta 700 064, India

Received 8 November 1996

Abstract. The effect of second-nearest-neighbour hopping on the transition temperature and the superconducting order parameter are investigated for d-wave superconductivity within the framework of the extended Hubbard model for both weak- and strong-correlation cases. The variation of the gap ratio with carrier concentration is studied. The isotope-shift exponent and the pressure coefficient of the transition temperature are investigated, taking into consideration isotopic mass and pressure dependences of the hopping and effective attractive interaction terms. The predicted variation of the isotope-shift exponent and the pressure coefficient with doping are in qualitative agreement with experimental findings for the high-T_c oxides.

1. Introduction

Superconductivity in narrow-band systems with an effective local non-retarded attractive interaction have been investigated extensively following the discovery of high-T_c oxide systems. Generally an extended Hubbard model in the small-U limit [1, 2] or a t–J (or t–J–v) model in the large-U limit [3–5] are considered for such studies. Previously we studied the superconducting phase diagram of an extended Hubbard model in both the large-U and small-U limits within the mean-field approximation for extended s-wave and d-wave pairing [2–4], and the variation of the gap ratio with doping for extended s-wave pairing [6]. For d-wave pairing the effect of second-nearest-neighbour hopping on the transition temperature and superconducting order parameter, and the variation of the superconducting gap ratio with doping have not been properly addressed so far. Recent experiments [7, 8] have revealed that the symmetry of the superconducting gap parameter in high-T_c systems is either of d-wave or of highly anisotropic s-wave type. Thus the study of different properties for a d-wave symmetry pairing has gained importance in the context of high-T_c systems.

High-T_c oxide systems exhibit an anomalous isotope effect. The isotope-shift exponent (α) is large for underdoped materials, decreases with doping, and attains a minimum at optimum doping [9]. The pressure coefficient of the transition temperature in high-T_c oxide systems (hole doped) is found to be large in the underdoped region and small at optimum doping. Negative values of the pressure coefficient have also been reported for the overdoped region [10]. An important question that might be asked is that of whether the observed isotope effect and the pressure effect on T_c may be obtained with a local pairing interaction for the d-wave pairing without considering any phonon-mediated mechanism.

The object of the present work is to study the effect of the second-nearest-neighbour hopping on the transition temperature, the superconducting order parameter, and the gap

0953-8984/97/193889+12$19.50

ratio for a tight-binding system with an effective intersite attractive interaction for both weak- and strong-correlation cases. The isotope effect and the pressure effect on T_c for the d-wave pairing are also studied.

2. The model Hamiltonian and the equation for the superconducting gap

A single-band extended Hubbard model with nearest- and second-nearest-neighbour hopping is given by

$$H = -\sum_{i,j,\sigma} t_{ij} c^+_{i\sigma} c_{j\sigma} + U \sum_i n_{i\uparrow} n_{i\downarrow} - v \sum_{i,j} n_i n_j - \mu \sum_i n_i \tag{1}$$

where t_{ij} is the hopping matrix element connecting sites i and j, which is equal to t (t_2) when i and j are nearest (second-nearest) neighbours. U is the on-site Coulomb repulsion, and v is an effective attraction between fermions at nearest-neighbour sites. $c^+_{i\sigma}$ ($c_{i\sigma}$) is the creation (annihilation) operator for an electron at site i with spin σ, n_i is the number operator, and μ is the chemical potential.

2.1. The weak-correlation case

In the weak-correlation cases one uses the standard Hartree-Fock (HF) approximation to tackle the two-body interaction term. An effective Hamiltonian for studying superconductivity is then obtained as

$$H = \sum_q (\epsilon_q - \mu) c^+_{q\sigma} c_{q\sigma} + \sum_q \{(v\Delta_1(q) - U\Delta_0) c_{-q\downarrow} c_{q\uparrow} + \text{HC}\} - C \tag{2}$$

where

$$\begin{aligned}\epsilon_q &= -2t(\cos(q_x a) + \cos(q_y a)) - 4t_2 \cos(q_x a)\cos(q_y a) \\ &= -2t(\cos(q_x a) + \cos(q_y a) + 2r\cos(q_x a)\cos(q_y a))\end{aligned}$$

for a square lattice (the Fock correction to the K.E. is neglected); $r = t_2/t$. The superconducting order parameters Δ_0 and $\Delta_1(q)$ are defined as

$$\Delta_0 = \langle c^+_{i\uparrow} c^+_{i\downarrow} \rangle \tag{3}$$

$$\Delta_1(q) = {\sum_j}' \langle c^+_{i\uparrow} c^+_{j\downarrow} \rangle e^{iq R_{ij}}. \tag{4}$$

The prime on the summation in equation (4) indicates that the summation is restricted to nearest-neighbour sites. The constant C compensates for the double counting in the interaction energy within the HF approximation.

The equations for the chemical potential and the superconducting order parameter at finite temperature may be obtained in the form

$$n = \frac{1}{N} \sum_q \left[1 - \frac{\xi_q}{E_q} \tanh\left(\frac{\beta E_q}{2}\right) \right] \tag{5}$$

$$\Delta_0 = \frac{1}{N} \sum_q (v\Delta_1(q) - U\Delta_0) \frac{1}{2E_q} \tanh\left(\frac{\beta E_q}{2}\right) \tag{6}$$

$$\Delta_{x(y)} = \langle c^+_{i\uparrow} c^+_{i\pm x(y)\downarrow} \rangle = \frac{1}{N} \sum_q (v\Delta_1(q) - U\Delta_0) \frac{1}{2E_q} \tanh\left(\frac{\beta E_q}{2}\right) \cos(q_{x(y)} a) \tag{7}$$

where

$$\xi_q = \epsilon_q - \mu \tag{8}$$

$$E_q = \sqrt{\xi_q^2 + (\Delta_q^g)^2} \tag{9}$$

$$\Delta_q^g = v\Delta_1(q) - U\Delta_0 \tag{10}$$

and n is the electron concentration. For d-wave pairing, $\Delta_x = -\Delta_y = \Delta$. In that case equations (2) and (3) yield $\Delta_0 = 0$, and the superconducting gap parameter becomes

$$\Delta_q^g = 2v\Delta(\cos(q_x a) - \cos(q_y a)). \tag{11}$$

From equation (7) one obtains the self-consistent solution for the gap parameter for d-wave pairing as

$$1 = \frac{1}{N}\sum_q v(\cos(q_x a) - \cos(q_y a))^2 \frac{1}{2E_q}\tanh\left(\frac{\beta E_q}{2}\right). \tag{12}$$

The corresponding equations for the transition temperature and the gap parameter at $T = 0$ are obtained from equation (12) as (in units of $k_B = 1$)

$$1 = \frac{1}{N}\sum_q v(\cos(q_x a) - \cos(q_y a))^2 \frac{1}{2\xi_q}\tanh\left(\frac{\xi_q}{2T_c}\right) \tag{13}$$

$$1 = \frac{1}{N}\sum_q v(\cos(q_x a) - \cos(q_y a))^2 \frac{1}{2\sqrt{\xi_q^2 + (\Delta_q^g)^2}}. \tag{14}$$

The superconducting gap, given in equation (11), has four nodes along the $k_x = k_y$ lines, and has d-wave symmetry. For a fixed filling, the maximum value of the gap is determined by the maximum value of $|(\cos k_x - \cos k_y)|$. For $0 \leqslant r \leqslant 1$, the maximum value of $|\cos(k_x) - \cos(k_y)|$ for a given chemical potential is given by

$$|\cos(k_x) - \cos(k_y)|_{max} = \begin{cases} 1 + \dfrac{1 + \mu/(2t)}{1 + 2r} & \text{for } \mu/(2t) \leqslant 2r \\ 1 + \dfrac{1 - \mu/(2t)}{1 - 2r} & \text{for } 2r \leqslant \mu/(2t) \leqslant 2 - 2r. \end{cases} \tag{15}$$

The maximum value of the superconducting gap for a given filling is obtained by determining Δ self-consistently from equation (14) and using the maximum value of $|\cos(k_x) - \cos(k_y)|$.

2.2. The strong-correlation limit

In the large-U limit, the extended Hubbard model in a projected space with no doubly occupied sites reduces to a t–J–v model which may be written in the X-operator representation [4]:

$$H = -\sum_{1,j,\sigma} t_{ij} X_i^{\sigma 0} X_j^{0\sigma} - \sum_{i,j,\sigma} \frac{J_{ij}}{4}(X_i^{\sigma\sigma} X_j^{\bar{\sigma}\bar{\sigma}} - X_i^{\sigma\bar{\sigma}} X_j^{\bar{\sigma}\sigma}) - \sum_{i,j} v_{ij} X_i^{\sigma\sigma} X_j^{\sigma'\sigma'} - \mu \sum_{i\sigma} n_{i\sigma} \tag{16}$$

where $J_{ij} = 4t_{ij}^2/U$ is the antiferromagnetic interaction induced by the strong correlation through virtual hopping. v_{ij} is an additional intersite attractive interaction as considered for the weak-correlation case.

$X_i^{\alpha\beta} = |\alpha\rangle_i\langle\beta|_i$ changes the state of the site i from $|\beta\rangle$ to $|\alpha\rangle$. $X_i^{\sigma 0}$ ($X_i^{0\sigma}$) and $X_i^{\sigma\sigma}$ are the creation (annihilation) and number operators, respectively, for an electron with spin

σ at a site i in a projected space with no doubly occupied sites. Following reference [4] the equations for the chemical potential and the superconducting gap parameter for d-wave pairing within the Hubbard-I decoupling approximation are given by

$$n = \frac{1}{N}\sum_q \left(\frac{1+x}{2}\right)\left[1 - \frac{\xi_q}{E_q}\tanh\left(\frac{\beta E_q}{2}\right)\right] \tag{17}$$

$$1 = \frac{1}{N}\sum_q \left(\frac{1+x}{2}\right)(J+v)(\cos(q_x a) - \cos(q_y a))^2 \frac{1}{2E_q}\tanh\left(\frac{\beta E_q}{2}\right) \tag{18}$$

where $x = 1 - n$ is the hole concentration in the system, and

$$\xi_q = \epsilon_q - \mu \tag{19}$$

$$\epsilon_q = \left(\frac{1+x}{2}\right)[-2t(\cos(q_x a) + \cos(q_y a)) - 4t_2 \cos(q_x a)\cos(q_y a)] \tag{20}$$

$$E_q = \sqrt{\xi_q^2 + (\Delta_q^g)^2} \tag{21}$$

$$\Delta_q^g = 2(J+v)\Delta(\cos(q_x a) - \cos(q_y a)). \tag{22}$$

In deriving equation (18) we have considered the effective attractive interactions to be non-zero only for nearest-neighbour sites. The equations for T_c and the superconducting gap parameter at zero temperature are obtained directly from equation (18). The summation over q is then replaced by an integration in q_x–q_y space in the thermodynamic limit, and the corresponding equations for the chemical potential, the transition temperature, and the superconducting gap are solved self-consistently.

3. The isotope-shift exponent

The basic parameters in the model which govern T_c are the hopping matrix elements, the effective attractive pairing interaction (v), and the chemical potential. If these parameters were to remain unchanged on isotopic substitution, there would be no change in T_c, and this would lead to zero isotope effect. Recently, experimental evidence for an increase in the effective mass of the charge carrier on heavier isotopic substitution has been obtained for the Y-123 system [11]. This suggests a decrease in the effective hopping of the charge carrier with increasing isotopic mass (M). In the La-214 system a change in the antiferromagnetic (AF) transition temperature has been observed on isotopic substitution, by Zhao and Morris [12]. They predicted a decrease in the AF interaction (J) with increasing M. The AF interaction in a strongly correlated system is induced by virtual hopping and is proportional to t^2. So a decrease in t with increasing M may be inferred from the results of reference [12]. Such a decrease in the effective hopping, with increasing M, may be realized if the charge carriers have polaronic character. In fact, Alexandrov [13] utilized this concept to explain the isotope effect in cuprates. However, for a pure polaronic superconductor, where the isotopic mass dependence occurs only in the effective hopping, the isotope-shift exponent is always negative [14].

For the effective attractive interaction (v), there is, so far, no experimental evidence of its variation with M. We assume here a variation of v and t with M, and study the role of these variations in the behaviour of the isotope-shift coefficient (α). In a previous paper we have made a similar study for the extended s-wave pairing [15], taking into consideration isotopic mass dependence of both t and v. It may be mentioned that if the effective attractive interaction (v) depends on the hopping integral (t), then v might change with M through its dependence on t, provided that t is a function of M as suggested by

reference [10]. In fact, within the antiferromagnetic scenario, the effective nearest-neighbour attraction is related to the antiferromagnetic interaction J [16], which is proportional to t^2. However, the mechanism of pairing in high-T_c oxide systems is not known, and isotopic mass dependence of the pairing interaction should be considered here as an assumption. Differentiating equation (13) for T_c with respect to M, one obtains the expression for the isotopic-shift exponent as

$$\alpha = -\frac{\partial \ln T_c}{\partial \ln M} = -\frac{\partial \ln t}{\partial \ln M} + \frac{1}{I_1}\left(\frac{\partial \ln t}{\partial \ln M} - \frac{\partial \ln v}{\partial \ln M}\right) \tag{23}$$

where

$$I_1 = \frac{1}{N}\sum_q \frac{v(\cos(q_x) - \cos(q_y))^2}{4T_c}\,\mathrm{sech}^2\left(\frac{\epsilon_q - \mu}{2T_c}\right). \tag{24}$$

Equation (23) shows directly that if $\partial \ln t/\partial M = \partial \ln v/\partial \ln M$, then the isotope-shift exponent $\alpha = -\partial \ln t/\partial \ln M$ is a constant, and does not depend on the chemical potential or the density of states.

In the strong-correlation limit the equation for the transition temperature is obtained directly from equation (18), and then the expression for the isotope-shift exponent can be written as

$$\alpha = -\frac{\partial \ln T_c}{\partial \ln M} = -\frac{\partial \ln t}{\partial \ln M} + \left(\frac{2}{1+x}\right)\frac{1}{I_2}\left(\frac{\partial \ln t}{\partial \ln M} - \frac{\partial \ln(J+v)}{\partial \ln M}\right) \tag{25}$$

where

$$I_2 = \frac{1}{N}\sum_q \frac{(J+v)(\cos(q_x) - \cos(q_y))^2}{4T_c}\,\mathrm{sech}^2\left(\frac{\epsilon_q - \mu}{2T_c}\right). \tag{26}$$

4. The pressure coefficient of the transition temperature

As pressure decreases the lattice spacing, it is expected that the hopping integral (t) and the attractive interaction (v) will increase on application of pressure. In high-T_c oxide systems, pressure also changes the carrier concentration of the system. Considering the above facts, differentiation of equation (13) for T_c with respect to pressure yields for the pressure coefficient

$$\gamma_p = \frac{\partial \ln T_c}{\partial p} = \frac{\partial \ln t}{\partial p} + \frac{1}{I_1}\left(\frac{\partial \ln v}{\partial p} - \frac{\partial \ln t}{\partial p}\right) + \frac{I_3}{I_1 I_4}\frac{\partial n}{\partial p} \tag{27}$$

where

$$I_3 = \frac{1}{N}\sum_q \frac{v(\cos(q_x) - \cos(q_y))^2}{\epsilon_q - \mu}\left[\frac{1}{2(\epsilon_q - \mu)}\tanh\left(\frac{\epsilon_q - \mu}{2T_c}\right) - \frac{1}{4T_c}\mathrm{sech}^2\left(\frac{\epsilon_q - \mu}{2T_c}\right)\right] \tag{28}$$

$$I_4 = \frac{1}{N}\sum_q \left(\frac{1}{2T_c}\right)\mathrm{sech}^2\left(\frac{\epsilon_q - \mu}{2T_c}\right) \tag{29}$$

and I_1 is given in equation (24).

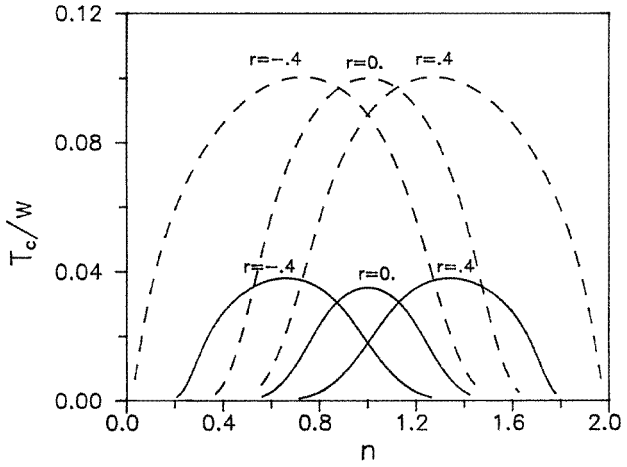

Figure 1. The variation of T_c/W with the carrier concentration (n) for different values of r ($=t_2/t$). Solid and dashed curves represent the results for $v/t = 1$ and 2, respectively.

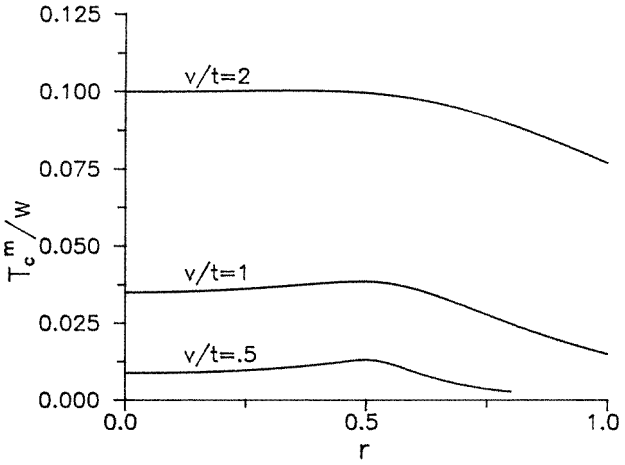

Figure 2. A plot of T_c^m/W versus r for different values of v/t.

5. Results and discussion

5.1. The role of the second-nearest-neighbour hopping as regards the superconducting phase diagram and the gap ratio

The transition temperature and the superconducting order parameter (Δ) for d-wave pairing are evaluated numerically from equations (13) and (14) as functions of the carrier concentration (n) for different values of v/t. It is evident from equation (13) that the value of T_c/t for a fixed filling depends only on the ratio v/t, rather than on the absolute values of v and t independently. In figure 1 we have shown the variation of T_c/W ($W = 4t$ is the half-bandwidth) with the carrier concentration (n) for two values of v/t and different values of $r = t_2/t$. It is well known that for $t_2 = 0$ the maximum in T_c (T_c^m) for d-wave pairing

occurs when the Fermi level lies at the middle of the band [1, 2], which corresponds to $n = 1$. This is evident from figure 1. For a square lattice the van Hove singularity (VHS) in the DOS for $t_2 = 0$ lies at the middle of the band. Thus, the Fermi level coincides with the VHS point at optimum doping, for which T_c is maximum. With the introduction of t_2, the VHS point in the DOS shifts by $4t_2$ from the centre of the new band; the total bandwidth, however, remains unchanged. As the VHS point shifts, the optimum doping concentration for the d-wave pairing also shifts, and $T_c = T_c^m$ is obtained when the chemical potential (the Fermi level) is close to the new VHS energy of the DOS. Figure 1 shows the shift of the T_c versus n plot with the introduction of t_2. When t_2 and t are of the same sign, the superconducting phase diagram shifts to higher values of n as compared to the $t_2 = 0$ case. If t_2 has the opposite sign, the phase diagram shifts to lower values of n. It may be mentioned that for the same magnitudes of t_2 but opposite signs, the T_c versus n curves are related by a mirror symmetry about $n = 1$. For $v/t = 2$, it is found that T_c^m remains almost unchanged as t_2 is switched from 0 to $0.4t$. A similar observation was made by Micnas *et al* [1] for the same value of v/t. For $v/t = 1$, T_c^m increases with the introduction of t_2. As t_2 is changed from 0 to $0.4t$, T_c^m rises by 8.5% for $v/t = 1$, while for $v/t = 4$ (not presented in the figure) we find that T_c^m decreases slightly for the same increase of t_2. Thus the effect of $r = t_2/t$ on T_c^m depends on the value of v/t. In figure 2 we plot the variation of T_c^m with r for different values of v/t. For $r \leqslant 0.5$, T_c^m increases with r for $v/t = 1$ and 0.5, while for $v/t = 2$ the change in T_c^m is negligible. For $r > 0.5$, T_c^m decreases with increasing r for all cases. The fractional rise in T_c^m up to $r = 0.5$ is higher for lower values of v/t.

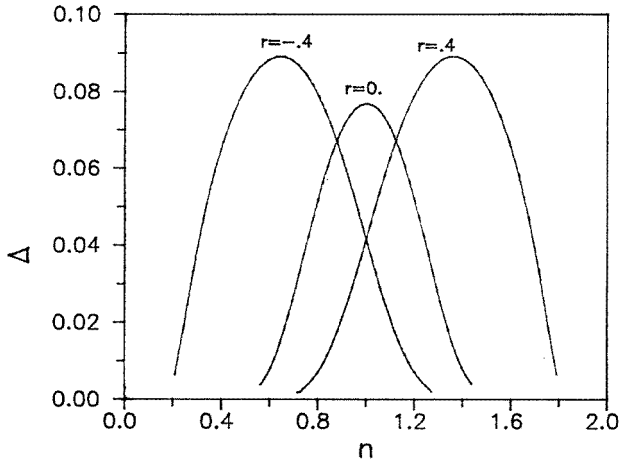

Figure 3. The variation of the superconducting order parameter (Δ) with carrier concentration (n) for different values of r ($=t_2/t$) for $v/t = 1$.

In figure 3 the variation of the superconducting order parameter (Δ) with n is presented for $v/t = 1$ for different values of r. It shows a similar variation to the T_c versus n curve, as expected.

In figure 4 we plot the maximum value of the superconducting gap ratio ($2\Delta_m^g/T_c$) against the carrier concentration for $v/t = 1$. For $r = 0$, the maximum value of $2\Delta_m^g/T_c$ is obtained as 4.39 for $\mu = 0$, i.e. at $n = 1$, where T_c has its maximum value. As the carrier concentration is changed from half-filling, the gap ratio decreases, reaches a minimum value, and then increases. For $r = 0.4$, the maximum value of the gap ratio is obtained as 4.79

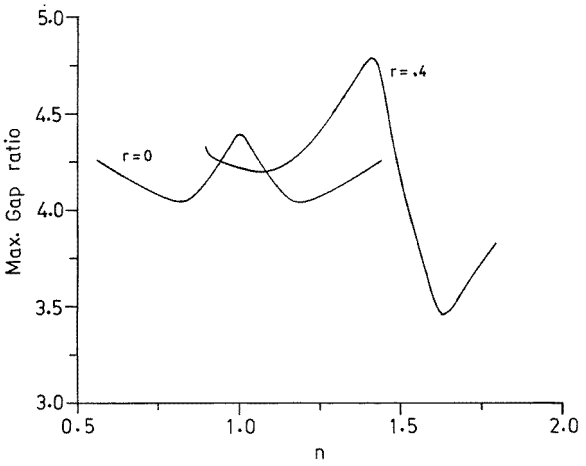

Figure 4. A plot of the gap ratio ($2\Delta_m^g/T_c$) versus n for $v/t = 1$ and $r = 0$ and 0.4.

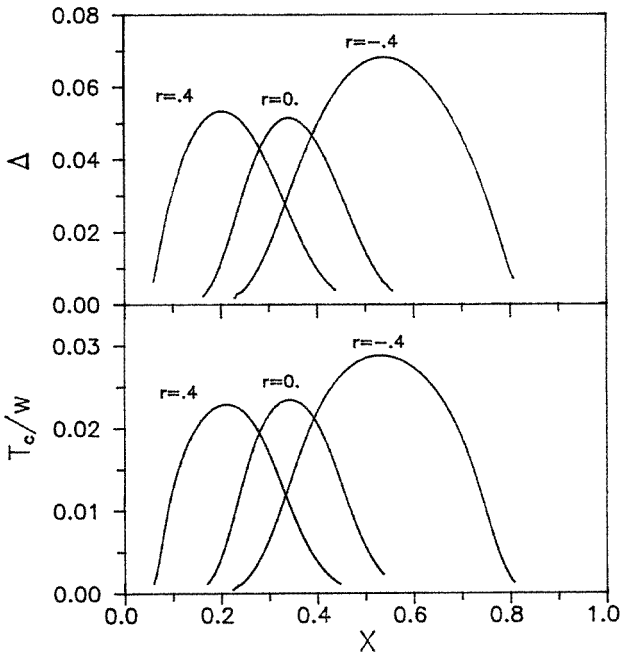

Figure 5. The variation of T_c/W and Δ with the hole concentration (x) for a strongly correlated system for $v/t = 1$ and different values of r ($=t_2/t$).

for a filling very near to the optimum doping (where T_c is maximum).

In figure 5 the variations of the transition temperature and the superconducting order parameter with the hole carrier concentration ($x = 1 - n$) are shown for the strong-correlation case. For $r = 0$, T_c and Δ are maximum for $\mu = 0$, which corresponds to $x = 1/3$ in the strong-correlation limit [3, 4]. With the introduction of r, the superconducting phase diagram shifts to higher or lower hole carrier densities, depending on the sign of r.

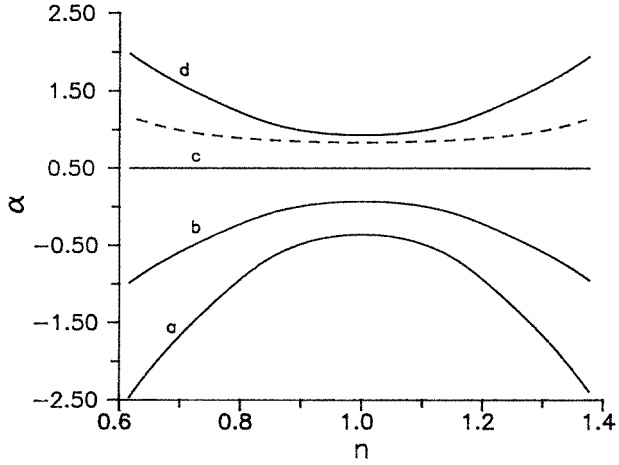

Figure 6. The variation of α versus n for $\partial \ln t/\partial \ln M = -0.5$. The solid curves are for $v/t = 1$. $\partial \ln v/\partial \ln M = 0, -0.25, -0.5$, and -0.75 for the curves a, b, c, and d respectively. Dashed curve: $v/t = 2$ and $\partial \ln v/\partial \ln M = -0.75$.

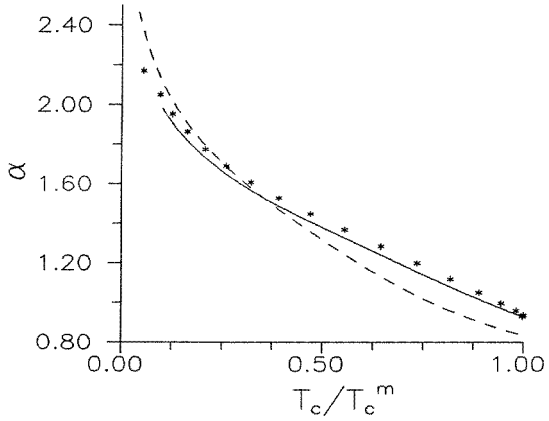

Figure 7. A plot of α versus T_c/T_c^m for $\partial \ln t/\partial \ln M = -0.5$ and $\partial \ln v/\partial \ln M = -0.75$. Solid curve: $v/t = 1$; dashed curve: $v/t = 2$; and $*$ represents the results for a strongly correlated system for $v/t = 1$.

Comparing figures 3 and 5, it seems that the sign of r has the opposite effect in shifting the phase diagram for the weak- and strong-correlation cases. However, this discrepancy is due to the fact that as the hole carrier density (x) decreases, the electron density (n) increases.

5.2. The isotope-shift exponent and the pressure coefficient

For determining the isotope-shift exponent and the pressure coefficient one has to select values of $\partial \ln t/\partial \ln M$, $\partial \ln v/\partial \ln M$ (or $\partial \ln(J+v)/\partial \ln M$ in the case of strong correlation), $\partial \ln t/\partial p$, $\partial \ln v/\partial p$, and $\partial n/\partial p$. Recent experiments indicate a change in the effective mass of the charge carrier due to the isotopic mass substitution in high-T_c systems [11]. Zhao and Morris [11] obtained a value of $\partial \ln(m^*)/\partial \ln M \sim 0.6$ for the Y-123 system,

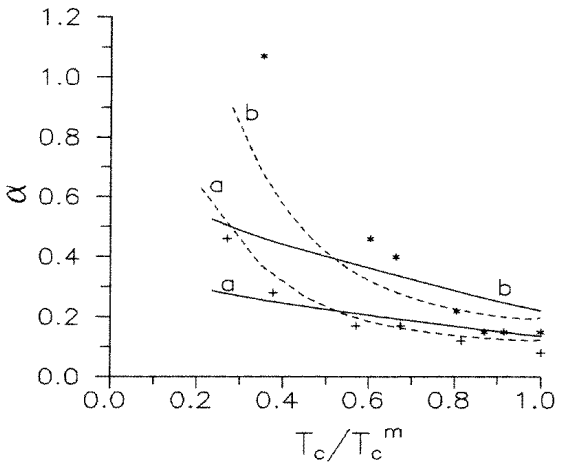

Figure 8. A plot of α versus T_c/T_c^m for $v/t = 1$ for different values of r $(=t_2/t)$. $\partial \ln t/\partial \ln M = -0.05$; (a) $\partial \ln v/\partial \ln M = -0.10$, (b) $\partial \ln v/\partial \ln M = -0.15$. Solid curves: $r = 0$; dashed curves: $r = 0.45$. $*$ and $+$ represent the experimental results for La-214 and Co-doped Y-123 systems, respectively (reference [9]).

where m^* is the effective mass of the charge carrier and M is the mass of the oxygen isotope. As the effective mass is inversely proportional to the hopping integral we take $\partial \ln t/\partial \ln M = -0.5$, guided by the above experiment. We assume $\partial \ln v/\partial \ln M$ to be a free parameter, and study the behaviour of α for different values of $\partial \ln v/\partial \ln M$ for a fixed value of $\partial \ln t/\partial \ln M$. For $\partial \ln t/\partial \ln M = \partial \ln v/\partial \ln M$, equation (23) yields that $\alpha = -\partial \ln t/\partial \ln M$. Under this condition, α becomes independent of the filling and is a constant as for BCS superconductors. In figure 6 we plot the variation of α with n for $\partial \ln v/\partial \ln M = -0.75, -0.5, -0.25$, and 0, for a fixed value of $\partial \ln t/\partial \ln M = -0.5$. The horizontal line of constant magnitude corresponds to α for $\partial \ln v/\partial \ln M = -0.5$. For $\partial \ln v/\partial \ln M = -0.75$, α is positive and large for both the underdoped and overdoped cases, and a minimum at optimum doping. For $\partial \ln v/\partial \ln M = -0.25$ and 0, α is negative in both the underdoped and overdoped regions, and has a maximum at optimum doping. For high-T_c oxide systems the general characteristics of α are that it is positive and large for underdoped systems, and passes through a minimum at optimum doping. Thus the nature of α for $\partial \ln v/\partial \ln M < \partial \ln t/\partial \ln M$ has a qualitative resemblance to that for the high-T_c oxide systems. In figure 7 we plot the variation of α with T_c/T_c^m for $\partial \ln v/\partial \ln M = -0.75$ with $\partial \ln t/\partial \ln M = -0.5$ and for $v/t = 1$ and 2. It is seen that α_{min} (the minimum value of α) is lower for a higher value of v. The values of α, determined from equation (25) for a strongly correlated system, are also shown in the same figure. It is found that the behaviour of α as a function of T_c/T_c^m is the same for both the strong- and weak-correlation cases, and is qualitatively consistent with the results for high-T_c oxide systems. The values of α shown in figures 6 and 7 are, however, much higher than the experimentally observed values for high-T_c oxide systems. From equation (23) it is evident that the magnitude of α is directly proportional to $\partial \ln t/\partial \ln M$ for a fixed ratio $(\partial \ln v/\partial \ln M)/(\partial \ln t/\partial \ln M)$. Hence the value of α can be reduced to the order of the experimental values ($\alpha_{min} \leqslant 0.1$) by taking appropriately small values of $\partial \ln t/\partial \ln M$ and $\partial \ln v/\partial \ln M$.

In figure 8 we show the variation of α with T_c/T_c^m for $v = t = 1$ and the weak-correlation case, taking $\partial \ln t/\partial \ln M = -0.05$, for two values of $\partial \ln v/\partial \ln M$ (-0.1 and

-0.15), and for $r = 0$ and 0.45. In the same figure, the experimental data points for La-214 and Co-doped Y-123 systems, as taken from reference [9], are given. It appears that there is a reasonable agreement between experimental data points and theoretical results for $r = 0.45$. It may be mentioned, however, that a quantitative comparison would be meaningful if accurate values of the (isotopic) mass-dependent parameters for the cuprates could be determined. Further, it is a matter of controversy whether such a minimal model as that considered here can describe the physics of cuprates. Our purpose is to just examine the behaviour of α for a model Hamiltonian which is widely studied in the context of high-T_c cuprates and to ascertain that a variation of α with doping, similar to that observed for cuprates, may be obtained if one assumes isotopic mass dependence of both the hopping and the attractive interaction.

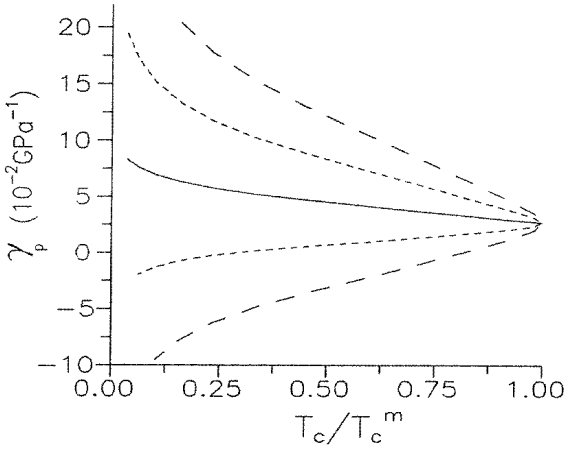

Figure 9. A plot of γ_p versus T_c/T_c^m for $v/t = 1$. The values of $\partial \ln t/\partial P$ and $\partial \ln v/\partial P$ are 1 and 2 in units of 10^{-2} GPa^{-1} respectively. The solid, short-dashed, and long-dashed curves are for $\partial n/\partial P = 0, 0.5$, and 1 in units of 10^{-2} GPa^{-1}.

To determine the values of the pressure coefficient we choose $\partial \ln t/\partial p = 1 \times 10^{-2}$ GPa^{-1} and $\partial \ln v/\partial p = 2 \times 10^{-2}$ GPa^{-1}. The pressure coefficient is studied for three values of $\partial n/\partial p$: 0, 0.5, and 1 in units of 10^{-2} GPa^{-1}. The former value is relevant for the La-214 system where the carrier concentration remains almost unaffected by pressure, while the latter values correspond to other high-T_c superconductors where the carrier concentration changes with pressure. In figure 9 we show the variation of the pressure coefficient (γ_p) with T_c/T_c^m. γ_p is large and positive for underdoped systems, and decreases as the carrier concentration increases up to optimum doping. For $\partial n/\partial p = 0$, γ_p is a minimum at optimum doping, and in the overdoped region it retraces the path as for the underdoped samples (this occurs because of the symmetry of γ_p around $n = 1$ in this case). A non-zero value of $\partial n/\partial p$ breaks the symmetry of γ_p around $n = 1$. For $\partial n/\partial p > 0$, γ_p is larger in the underdoped region, and the rate of fall of γ_p with carrier concentration is higher than in the $\partial n/\partial p = 0$ case. In the overdoped region, γ_p is negative provided that $\partial n/\partial p$ is appreciable. In high-T_c oxides the pressure coefficient is positive and large for underdoped samples, and decreases with increasing carrier concentration. Thus the behaviour of γ_p obtained in our study agrees qualitatively with the experimental results for high-T_c oxide systems.

6. Summary

We have investigated the d-wave superconductivity in the framework of the extended Hubbard model, with nearest-neighbour (t) and second-nearest-neighbour (t_2) hopping, within mean-field approximations—namely the HF approximation for the weak-correlation case and the X-operator technique for the strong-correlation case. For $t_2 = 0$ the maximum in T_c and Δ occurs at zero chemical potential, which corresponds to $n = 1$ for the weak-correlation case and $x = 1/3$ for the strong-correlation case [4]. With the introduction of t_2, the superconducting phase diagram shifts to the higher- or lower-electron-concentration side depending on whether the sign of t_2/t is positive or negative. It is found that the effect of t_2 on the maximum transition temperature (T_c^m) depends on the values of t_2 and v/t. For low values of v/t, T_c^m rises with t_2 for $|t_2/t| \leqslant 0.5$. For higher values of t_2, T_c^m decreases with increasing t_2. The maximum superconducting gap ratio is found to increase from 4.39 to 4.79 as t_2 is increased from 0 to $0.4t$ for $v/t = 1$.

The isotope-shift exponent in this model is examined by assuming isotopic mass dependence of t and v. For $\partial \ln v/\partial \ln M < \partial \ln t/\partial \ln M$, the behaviour of the isotope-shift exponent is found to be similar in nature to that of high-T_c oxide systems. The isotope-shift exponent is large for underdoped systems, and attains a minimum at optimum doping. It is interesting to note that we obtain very similar variations of α with T_c for the weak- and strong-correlation cases. For large values of t_2, relevant for high-T_c cuprates [7], the theoretical curves for α agree reasonably well with the experimental data points.

The pressure coefficient is investigated by assuming pressure dependence of t, v, and n. The pressure coefficient is found to be large for underdoped systems, and low at optimum doping. For $\partial n/\partial p > 0$, the pressure coefficient may be negative in the overdoped region. These results are qualitatively consistent with the experimental findings for high-T_c systems.

References

[1] Micnas R, Ranninger J and Robaszkiewicz S 1990 *Rev. Mod. Phys.* **62** 113
[2] Ray D K, Konior J, Oles A M and Das A N 1991 *Phys. Rev.* B **43** 5606
[3] Das A N, Ghosh B and Choudhury P 1989 *Physica* C **158** 311
[4] Das A N, Konior J, Ray D K and Oles A M 1991 *Phys. Rev.* B **44** 7680 and references therein
[5] Dagotto E 1994 *Rev. Mod. Phys.* **66** 763
[6] Das A N, Sarkar S and Choudhury P 1993 *Phys. Rev.* B **48** 16 673
[7] Wollman D A, Van Harlingen D J, Lee W C, Ginsberg D M and Leggett A J 1993 *Phys. Rev. Lett.* **71** 2134
Tsuei C C, Kirtley J R, Chi C C, Yu-Jahnes L S, Gupta A, Shaw T, Sun J Z and Ketchen M B 1994 *Phys. Rev. Lett.* **73** 593
[8] Shen Z X *et al* 1993 *Phys. Rev. Lett.* **70** 1553
[9] Franck J P 1994 *Physical Properties of High-Temperature Superconductivity* vol IV, ed D M Ginsberg (Singapore: World Scientific) p 189
[10] Schilling J S and Klotz S 1992 *Physical Properties of High-Temperature Superconductivity* vol III, ed D M Ginsberg (Singapore: World Scientific) p 59
[11] Zhao Guo-meng and Morris D E 1995 *Phys. Rev.* B **51** 16 487
[12] Zhao Guo-meng, Singh K K and Morris D E 1994 *Phys. Rev.* B **50** 4112
[13] Alexandrov A S 1992 *Phys. Rev.* B **46** 14 932
[14] Banerjee S, Das A N and Ray D K 1996 *Phys. Lett.* **214A** 89
[15] Banerjee S and Das A N 1996 *J. Phys.: Condens. Matter* **8** 11 131
[16] Dagotto E, Nazarenko A and Moreo A 1995 *Phys. Rev. Lett.* **74** 310